analytical chemistry

Article

pubs.acs.org/ac

Attractive Design: An Elution Solvent Optimization Platform for Magnetic-Bead-based Fractionation Using Digital Microfluidics and Design of Experiments

Nelson M. Lafrenière,[†,⊥] Jared M. Mudrik,[†,⊥] Alphonsus H. C. Ng,[‡] Brendon Seale,[†] Neil Spooner,[§] and Aaron R. Wheeler*[,†,‡]

[†]Department of Chemistry, University of Toronto, 80 St George Street, Toronto, Ontario M5S 3H6, Canada

[‡]Institute of Biomaterials and Biomedical Engineering, 164 College Street, Toronto, Ontario M5S 3G9, Canada

[§]Platform Technologies and Science Drug Metabolism and Pharmacokinetics, GlaxoSmithKline Research and Development, Ware, Hertfordshire SG12 0DP, United Kingdom

ABSTRACT: There is great interest in the development of integrated tools allowing for miniaturized sample processing, including solid phase extraction (SPE). We introduce a new format for microfluidic SPE relying on C18-functionalized magnetic beads that can be manipulated in droplets in a digital microfluidic platform. This format provides the opportunity to tune the amount (and potentially the type) of stationary phase on-the-fly, and allows the removal of beads after the extraction (to enable other operations in same device-space), maintaining device reconfigurability. Using the new method, we employed a design of experiments (DOE) operation to enable automated on-chip optimization of elution solvent composition for reversed phase SPE of a model system. Further, conditions were selected to enable on-chip fractionation of multiple analytes. Finally, the method was demonstrated to be useful for online cleanup of extracts from dried blood spot (DBS) samples. We anticipate this combination of features will prove useful for separating a wide range of analytes, from small molecules to peptides, from complex matrices.

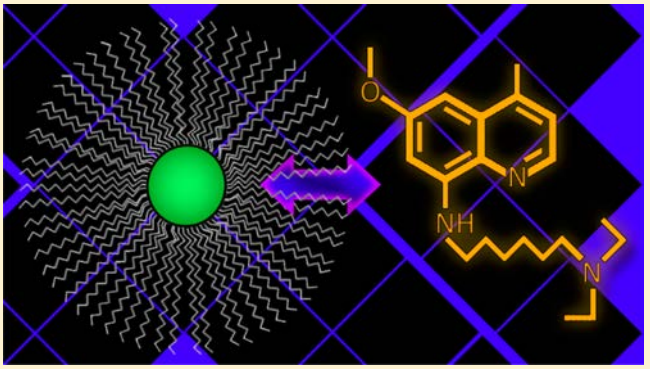

Solid phase extraction (SPE) is a versatile extraction technique in which analytes partition between two phases: a liquid solvent and a solid sorbent.[1] In a typical SPE experiment, the analyte of interest is adsorbed onto the solid phase (and the original solvent is washed away) and then is eluted in a more concentrated and purified form. SPE is widely used in diverse fields ranging from pharmacokinetics[2] and forensics,[3,4] to environmental and biological trace analysis,[5−8] and food analysis.[9,10]

Recently, there has been great interest in the use of microfluidics-based "lab on a chip" technologies for the integration of sample delivery, separation, and detection on-chip.[11] Microfluidic systems are particularly attractive for applications involving precious samples such as rare environmental microbe specimens,[12] core needle biopsies,[13] and samples to be collected and analyzed autonomously.[14] Many different formats of microchannel-based devices designed for SPE have been reported, including channels coated with stationary-phase materials,[15] channels packed with beds of beads,[16−18] channels incorporating porous membranes,[19] and channels bearing porous polymer monoliths (PPMs).[20] Microchannel-based methods are useful for many applications (and are particularly well suited for integration with separations), but they are not a universal solution appropriate for all applications; for example, complexities related to "world-to-chip" interfacing make microchannel-based devices challenging to use when screening many different solvents and elution conditions for method optimization.

Digital microfluidics (DMF) is an alternative to microchannels for miniaturized analysis. In DMF, discrete droplets of liquid are manipulated via electrodynamic forces on the surface of an insulated two-dimensional array of electrodes.[21,22] Although sharing some features with microchannels, DMF is particularly well suited for applications incorporating solid materials into analytical workflows[23−27] (as there is no risk of clogging) and for applications requiring the generation of arbitrary mixtures on device (e.g., serial dilutions[28] and tunable gel compositions[29]). As a consequence of the flexibility with which liquids can be automatically merged, mixed, and dispensed using DMF, we hypothesized that it would be a useful platform for on-chip optimization of solvent conditions for SPE.

Received: December 17, 2014
Accepted: March 3, 2015
Published: March 11, 2015

DOI: 10.1021/ac504697r
Anal. Chem. 2015, 87, 3902−3910

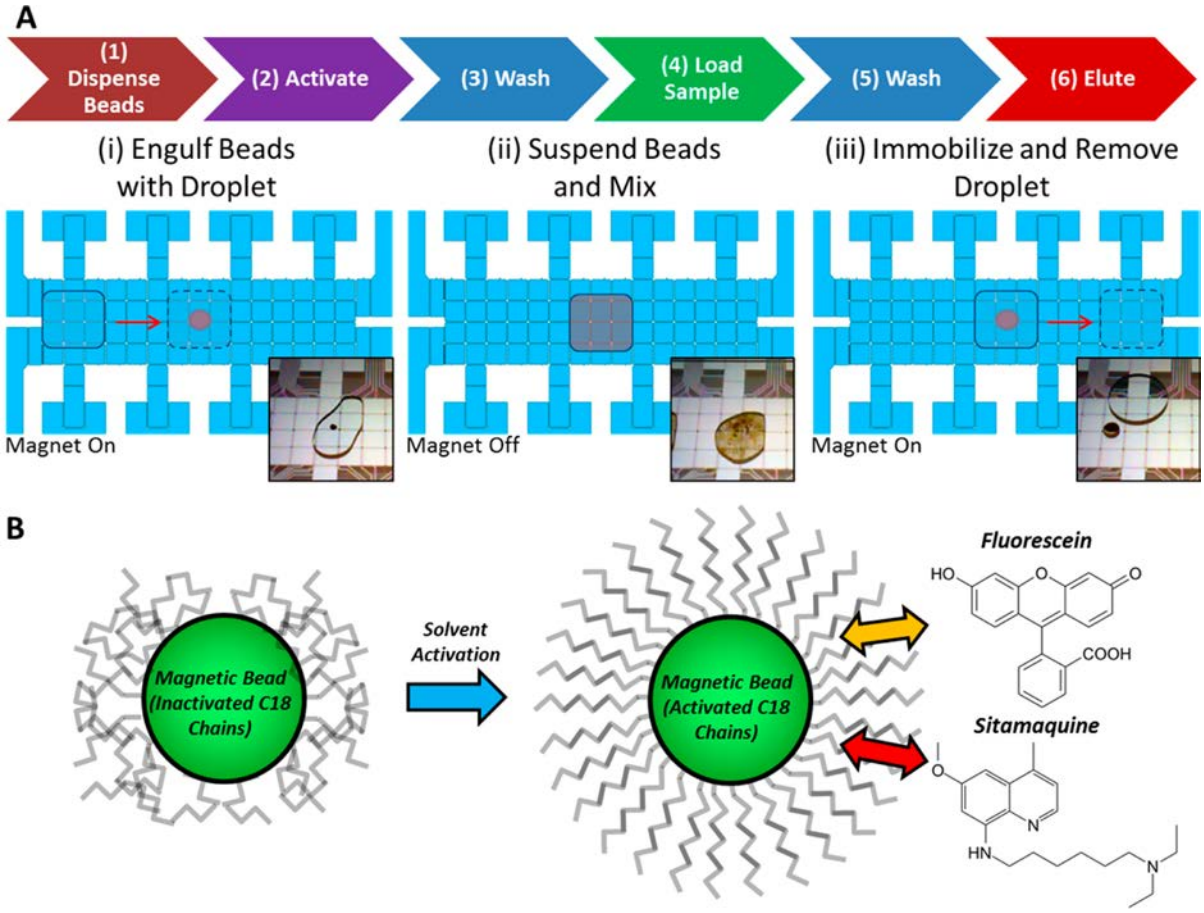

Figure 1. DMF-magnetic-bead SPE. (A, Top) process flow diagram for the six-step SPE method: (1) dispense, (2) activate, (3) wash, (4) load, (5) wash, and (6) elute. (Bottom) cartoon (main panels) and pictures (insets) depicting the three fundamental operations employed in steps 2–6: (i) engulf beads with droplet, (ii) suspend beads and mix, and (iii) immobilize and remove solvent. In i and iii, the magnetic lens is engaged by positioning it close to the device; in ii, the magnetic lens is disengaged by moving it away from the device. (B) Schematic illustrating solvent activation of C18 structures (step 2 above) and interaction of analytes fluorescein and sitamaquine with the activated structure (step 4 above).

The first techniques for performing SPE on DMF were recently reported,[30,31] the first of which used PPMs with C12 alkyl moieties (for reversed phase applications) as a solid phase and the second used sulfonate-functionalized PPMs for strong cation exchange (SCX) SPE. Droplets were driven to and from the stationary and permanent PPM structures to enable the various steps required for extraction (equilibration/activation, loading, rinsing, eluting, etc.). PPMs are a useful format for SPE, but they have some disadvantages, including being static: once formed, their size, volume, and porosity cannot be changed. An ideal SPE system would have a reconfigurable stationary phase system that could be tuned depending on the application.

Here we report a new digital microfluidic method for SPE, using magnetic beads functionalized with C18 alkyl moieties for reversed phase fractionation. We propose that this represents an improvement over previous work with PPMs: the C18-coated magnetic beads enable DMF-based SPE while (a) providing the opportunity to tune the amount (and potentially the type) of sorbent on-the-fly, and (b) allowing the removal of beads after extraction (to enable other operations in same device-space), maintaining device reconfigurability. Furthermore, this innovation enables demonstration of a unique capability of DMF, (c) fully automated on-chip optimization of the elution solvent composition. Finally, upon optimization, conditions were selected to allow for (d) on-chip fractionation of multiple analytes. We anticipate this combination of features (a–d) will prove useful for separating a wide range of analytes, from small molecules to peptides, from complex matrices.

EXPERIMENTAL SECTION

Reagents and Materials. Unless otherwise specified, all chemicals were purchased from Sigma-Aldrich (Oakville, Ontario) and were used without modification. HPLC-grade acetonitrile and methanol were purchased from Fisher Scientific (Ottawa, Ontario). Cleanroom supplies included Parylene C dimer from Specialty Coating Systems (Indianapolis, Indiana) and Teflon AF from Dupont (Wilmington, Delaware). Magnetic beads (1 μm dia.) with C18 aliphatic functionality (SiMAG-Octadecyl) were purchased from Chemicell GmbH (Berlin, Germany). Sitamaquine and $^{2}H_{10}$-sitamaquine were graciously provided by GSK (Stevenage, United Kingdom).

DMF Device Fabrication and Operation. DMF device bottom plates were formed bearing a 15-by-4 array of driving electrodes (2 × 2 mm) and 8 reservoir electrodes (16 × 6 mm). To form the electrode array, glass slides precoated with chromium (200 nm) and photoresist (AZ1500, 530 nm) (Telic Co., Santa Clarita, California) were patterned via photolithography and wet etching in the Toronto Nanofabrication Centre cleanroom at the University of Toronto as described previously.[32] The finished DMF bottom plates were coated

DOI: 10.1021/ac504697r
Anal. Chem. 2015, 87, 3902–3910

with a layer of Parylene C dielectric (7 μm) by vapor deposition (Specialty Coating Systems) and spin coated with a layer of Teflon AF (50 nm, 30 s, 1000 rpm) followed by postbaking on a hot plate (160 °C, 10 min).

DMF top plates were formed from indium tin oxide (ITO)-coated glass (Delta Technologies Ltd., Stillwater, Minnesota) spin coated with a layer of Teflon AF (50 nm, as above). DMF top and bottom plates were assembled by sandwiching them together with three layers (270 μm) of double-sided tape (3M, London, Ontario) as spacers. An automated control system with integrated moveable magnetic lens (described in detail elsewhere[33]) was used to actuate droplets by applying electrical potentials (100−120 V_{RMS}, 10 kHz) to successive DMF electrodes. To immobilize magnetic beads, a magnetic lens was moved vertically (by means of the integrated step-motor) beneath the DMF device.

Solid-Phase Extraction. A six-step method (Figure 1A top) was developed to implement solid-phase extraction using magnetic beads. At the beginning of each experiment, C18 magnetic beads were prepared in aqueous suspension (5 mg/mL or ~9.0×10^9 beads/mL) and were pipetted onto a device in 10 μL aliquots (step 1), each forming a "bed" of beads. To remove liquid from beads (for this step and in all stages of the extraction process), the automated control system's magnetic lens was engaged, immobilizing the beads on the device surface, allowing the liquid to be moved away via DMF actuation. The magnetic beads were activated with acetonitrile (10 μL droplet, step 2) and rinsed with water (10 μL droplet, step 3) on-device. Extractions then proceeded with sample loading and incubation (10 μL droplet, 5 min, step 4) with droplet mixing via DMF actuation, washing twice with water (2 × 10 μL droplets, step 5), and elutions with an appropriate solvent (10 μL droplet, step 6). Each of steps 2−6 comprised three operations: (i) engulfing beads in solvent, (ii) mixing beads within solvent, and (iii) removing solvent from beads (Figure 1A bottom).

Loading Capacity and Equilibrium Characterization. To measure the loading capacity of C18 magnetic beads, aqueous samples of fluorescein (10 μL droplet, 0.1% trifluoroacetic acid, TFA) of varying concentrations (0.01, 0.1, 1, 10, and 100 mg/mL) were loaded onto single beds of C18 magnetic beads and incubated with mixing for 5 min. The sample droplets were driven away from the beads and the concentrations of remaining (unadsorbed) fluorescein in the droplets were measured off-chip with a plate reader (PheraStar, BMG Labtech, Durham, NC) (λ_{ex}, 480 nm; λ_{em}, 520 nm). Experiments were performed in triplicate for each concentration, with calibrants prepared from fluorescein in 0.1% TFA.

To characterize loading equilibrium of sitamaquine, the above experiment was repeated in triplicate with aqueous sitamaquine (10 μL droplet, 1 μg/mL). The concentration of sitamaquine remaining in the recovered sample droplet was quantified using electrospray ionization tandem mass spectrometry (ESI-MS/MS, LTQ, Thermo Scientific, Waltham, MA) operating in selected reaction monitoring (SRM) mode. Prior to analysis, each eluate (~10 μL droplet) was combined with a 10 μL aliquot of internal standard ($^2H_{10}$: sitamaquine, 500 ng/mL in acetonitrile) and diluted to a volume of 100 μL with acetonitrile/water (1:1, v/v) containing 0.1% formic acid off-chip. Samples were analyzed in positive ion mode, with the applied spray voltage varied between 1.2 and 1.5 kV. The flow rate of the syringe pump and capillary temperature were kept constant at 0.5 μL/min and 350 °C, respectively. High purity (99.995%) helium gas was used for collision activated dissociation, and SRM mass transitions of 344 to 271 and 354 to 271 were monitored for sitamaquine and its internal standard (IS). Spectra were collected as an average of ten acquisitions using Thermo Finnigan Xcalibur software (Version 2.0). The ratios of peak intensities (sitamaquine:IS) of the product ions were recorded and used for quantification. The logarithm of the loading equilibrium constant (log K) was then estimated using eq 1:

$$K = \frac{n_s}{n_m} \times \frac{V_m}{V_s} \quad (1)$$

where n_s represents the moles of analyte in the stationary phase, n_m the moles of analyte in the mobile phase, V_m the volume of the mobile phase, and V_s the volume of the stationary phase.

On-Chip Solvent Composition. Using a programmed sequence of DMF actuation steps, mixtures of solvents were composed automatically on-device. Reservoirs were filled with neat solvents (water, acetonitrile and methanol). Solvent droplets the size of a single actuation electrode (unit droplets, 2.5 μL) were dispensed from reservoirs, and combined and mixed in the desired proportions to form appropriate solvent mixtures for elution experiments.

Design of Experiments for Elution Solvent Optimization. Design of experiments was performed using JMP (SAS, Cary, North Carolina). A simplex-centroid model was used to choose the required experimental data points for combinations of acetonitrile, methanol, and water. As a result of this model, seven elution solvent combinations were chosen: the three neat solvents, the three binary mixtures (1:1 proportions, v/v), and the 1:1:1 (v/v) ternary mixture of the solvents. Extractions of separate aqueous solutions of sitamaquine (10 μL droplet,1 μg/mL) and angiotensin I (10 μL droplet, 50 μg/mL) were performed as described above, eluting with the solvent mixtures generated on-chip (prescribed by the model). ESI-MS/MS was used to quantify recovered sitamaquine (as described above) and ESI-MS was used to quantify recovered angiotensin I. For the latter, each eluate (~10 μL droplet) was combined with 10 μL of internal standard (bradykinin, 10 μg/mL in acetonitrile/water, 1:1, v/v with 0.1% formic acid) and diluted to a volume of 100 μL with acetonitrile/water (1:1, v/v) containing 0.1% formic acid off-chip. Samples were analyzed in positive ion mode, with applied spray voltage varied between 1.2 and 1.5 kV, the flow rate of the syringe pump and capillary temperature were kept constant at 0.5 μL/min and 200 °C, respectively. The triply protonated peaks ($[M + 3H]^{3+}$) of angiotensin I (433 m/z) and bradykinin (354 m/z, IS) were monitored, and the ratios of peak intensities (analyte:IS) were used for quantification. Spectra were collected as an average of ten acquisitions using Thermo Finnigan Xcalibur software (Version 2.0).

The experimental data collected for sitamaquine and angiotensin were fit with a three-component (i, j, k) special cubic model, which involves the same number of terms as there are points in the associated simplex centroid design (eq 2):

$$\hat{y} = \sum_i b_i x_i + \sum_i \sum_{<j} b_{ij} x_i x_j + \sum_i \sum_{<j} \sum_{<k} b_{ijk} x_i x_j x_k \quad (2)$$

where $\hat{y}$ is the predicted extraction efficiency, x_n ($n = i, j, k$) is the solvent fraction, b_i is the linear blending coefficient, b_{ij} is the coefficient representing binary effects, and b_{ijk} is the coefficient representing ternary effects. For comparison, a web-based[34] Abraham solvation equation[35] calculator was used to predict the solubilities of sitamaquine (molar volume 332.3 ± 3.0 cm^3,

DOI: 10.1021/ac504697r
Anal. Chem. 2015, 87, 3902−3910

molar refractivity 108.7 ± 0.3 cm^3, SMILES CCN(CC)-CCCCCCNc1cc(cc2c1nccc2C)OC) in water, acetonitrile, and methanol.

Evaluation of Extraction Efficiency. The extraction efficiency of C18 magnetic beads on DMF was compared to that of commercial C18 ZipTips (Millipore, Toronto, Ontario). DMF-based extractions were performed with sitamaquine and angiotensin I as described above, eluting each sitamaquine sample in a 10 μL droplet of neat methanol and each angiotensin I sample in a 10 μL droplet of 1:1 acetonitrile:-water. The same solvents were used to extract these analytes using C18 ZipTips following the manufacturer's instructions. Briefly, C18 ZipTips were activated by aspirating and expirating acetonitrile (10 μL), washed by aspirating and expirating water (10 μL), loaded with sample (10 μL) by repeatedly (5×) aspirating and expirating the sample, then rinsed twice by aspirating and expirating volumes of water (10 μL). Finally, two elution steps were performed with the appropriate solvent mixture, repeatedly (10×) aspirating and expirating two volumes of elution solvent. Eluted sitamaquine and angiotensin I concentrations were quantified via ESI-MS/MS and ESI-MS, respectively, as described above.

Sample Fractionation. An aqueous mixture of sitamaquine and angiotensin I (1 μg/mL and 50 μg/mL, respectively) was loaded and extracted via DMF actuation using C18 beads as described above. The first elution step was performed with methanol and the second elution step was performed with 1:1 acetonitrile:water (v/v). The two eluted fractions were collected and individually analyzed for sitamaquine and angiotensin I via ESI-MS/MS and ESI-MS, respectively (as above). For this analysis, each eluate (∼10 μL droplet) was spiked with a 10 μL aliquot of aqueous IS solution (500 ng/mL $^2H^{10}$-sitamaquine, 10 μg/mL bradykinin) and diluted to a volume of 100 μL with acetonitrile/water (1:1, v/v) containing 0.1% formic acid off-chip, before being analyzed as described above. In this case, the doubly protonated peak of bradykinin (531 m/z) was used for quantification instead of the triply protonated peak (354 m/z).

Dried Blood Spot Extraction and Cleanup. Dried blood spots (DBSs) were prepared by spotting 15 μL aliquots of human whole blood (BioChemed Services, Winchester, Virginia) containing 5 μg/mL sitamaquine onto paper cards (PerkinElmer 226 Sample Collection Cards, Greenville, South Carolina). After drying, a 2 mm biopsy punch was used to cut out a circular punch for extraction. In each experiment, a DBS punch was placed on a DMF device and was extracted into methanol (30 μL, 5 min) using methods similar to those reported previously.[36] Following extraction, a unit droplet (2.5 μL) of extract was split off for C18 bead cleanup, and the remainder of the extract was removed from the device to be used as a control. The unit droplet of DBS extract was combined with a water droplet (22.5 μL) and extracted using a bed of C18 beads following the procedure outlined above (eluting into neat methanol). Off-chip, the eluate was diluted to 100 μL with 1:1 acetonitrile:water with 0.5% formic acid for mass spectrometric analysis. For comparison, 2.5 μL aliquots of raw DBS extract (without C18 cleanup) were diluted to 10 μL with methanol, then to 100 μL with 1:1 acetonitrile:water with 0.5% formic acid. Samples were analyzed by ESI-MS/MS with direct infusion at 2 μL/min into an API 4000 Triple Quadrupole MS/MS (AB Sciex, Concord, Ontario) where they were analyzed in positive ion mode with an applied spray voltage of 5 kV. MS/MS spectra were collected as averages of 12 scans for the 344−271 m/z transition.

RESULTS AND DISCUSSION

DMF-Magnetic Bead-SPE. There are two previous examples of solid phase extraction (SPE) implemented by digital microfluidics,[30,31] both relying on stationary porous polymer monolith discs. Here, we sought to improve upon these techniques by taking advantage of another recent development in digital microfluidics: the use of magnetic particles for immunoassays,[23,33,37−42] cell manipulation,[43,44] and protein immuno-depletion.[45] Magnetic particles are useful in a wide range of settings, as they can form high surface-area sorbents for heterogeneous applications, but also their positions can be manipulated relative to that of the solvent (or other system components) using magnetic fields. Here, we used an integrated instrument with a motorized magnetic lens (developed originally for immunoassays, described in detail previously[33]) that allows for reversible immobilization of magnetic particles to the surface of DMF devices, to explore whether this technique is suitable for reversed-phase solid-phase extraction.

In this work, we used 1 μm diameter C18-functionalized magnetic particles to develop a six-step SPE method, in which (1) a bed of beads (estimated to be 9×10^7 beads, 1×10^{-12} cm^3) is formed, (2) the C18 functionality of the beads is activated with an appropriate solvent, (3) the beads are washed, (4) the sample is loaded and incubated on the beads, (5) the beads are washed again, and (6) the analytes are eluted from the beads (Figure 1A, top). These steps are achieved through a repeating series of three operations: (i) a droplet is dispensed, driven to the beads, and moved such that they become dispersed, (ii) the suspension is actively mixed and incubated, and (iii) the beads are immobilized and spent solution (supernatant) driven away (Figure 1A, bottom). The entire six-step extraction process can be completed in ∼12 min (Table 1) with up to three extractions performed in parallel with the current implementation of the device, yielding a throughput of 15 samples/h. Although commercially available systems such as 96-well SPE plates offer higher throughput (96 samples/h[46]), this benefit is somewhat offset by the costs associated with solvent consumption and maintenance of robotic fluid handling systems.

Table 1. Approximate Duration (in seconds) for Each Step in the DMF-SPE Protocol

step	approximate duration (s)
1 − dispensing of bead bed	10
2 − solvent activation	30
3 − washing	30
4 − sample loading	300
5 − washing (2×)	60
6 − elution	300

In initial experiments, it was found that the Pluronic droplet-additives (amphiphilic coblock-polymers of poly(ethylene oxide) and poly(propylene oxide)) that are often used in DMF to reduce nonspecific adsorption[47,48] to the fluoropolymer-coated device surfaces (which can impede droplet movement), were incompatible with this process, resulting in a significant drop in extraction performance, likely caused by micellar encapsulation of hydrophobic analytes and/or coating

DOI: 10.1021/ac504697r
Anal. Chem. 2015, 87, 3902−3910

of the particle surfaces with adsorbed pluronic. Thus, pluronic additives were not used in the work reported here; this was not observed to present any hindrance to droplet movement or result in appreciable sample loss. In the future, depending on the application, it may be necessary to explore alternate antifouling strategies that are compatible with C18 magnetic beads (potentially including the use of DMF device coatings designed to resist fouling[49]).

Loading Capacity, Saturation, and Equilibrium. The new DMF-magnetic bead-SPE method was evaluated for loading capacity over a wide range of concentrations of a model analyte (fluorescein), by evaluating the fluorescence intensity of analyte in the supernatant (the droplet at the end of step 4, above) relative to that of the unextracted sample. As shown in Figure 2A, ~10% of the sample remained unbound

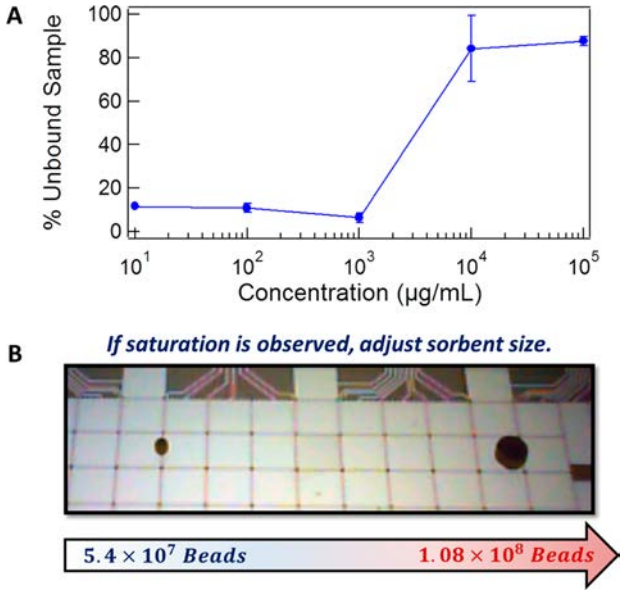

Figure 2. Loading capacity and bead bed size in DMF-magnetic bead-SPE. (A) Plot of the ratio of fluorescence intensity of supernatant droplets (postextraction) relative to that of stock solution as a function of fluorescein concentration. All experiments used sorbent beds formed from 10 μL of bead suspension (~9×10^7 beads, ~9×10^{-5} cm^3). Error bars represent ±1 SD, n = 3. (B) Pictures of sorbent beds formed from 6 μL (left) (~5.4×10^7 beads, ~5×10^{-5} cm^3), or 12 μL (right) (~1.08×10^8 beads, ~1×10^{-4} cm^3) of bead suspension

for initial concentrations of 1−1000 μg/mL, indicating that these quantities of fluorescein loaded successfully without saturation. At concentrations of 10 mg/mL and higher, the magnetic beads became saturated, resulting in a drop in loading with >80% of sample remaining unbound.

Saturation in solid phase extraction is a phenomenon that can be costly in terms of time and funds (i.e., new experiments must be repeated with new SPE cartridges with larger sorbent beds). This problem is magnified in microfluidic SPE systems: the relative cost and complexity of devices with permanent, single-size sorbent beds (whether implemented in microchannels[15−20] or by DMF[30,31]) makes the process of disposing and replacing them unattractive. This problem can be solved using the methods described here; on a given device, the sorbent size can be determined on-the-fly. As shown in Figure 2B, it is trivial to form sorbent beds containing different numbers of beads (in this example, ~5.4×10^7 on the left, and ~1.08×10^8 on the right). The flexibility and adaptability of using magnetic beads on DMF could thus be advantageous in applications in which devices are precious or must be reused.

After establishing convenient (generic) working conditions for the new procedure, we turned our attention to the experimental antimalarial drug sitamaquine, to serve as a model for small-molecule pharmaceutical analytes. The equilibrium constant for adsorption of sitamaquine to the stationary phase was estimated by extracting a 1 μg/mL solution and measuring the fraction of (unretained) analyte remaining in the sample droplet (by tandem mass spectrometry) postextraction (1.45%). This data, along with the known volume of the mobile phase (10 μL) and the estimated volume of the stationary phase (6.03×10^{-7} mL, assuming the stationary phase on a single magnetic bead is a shell with uniform thickness equivalent to the approximate length of an octadecyl alkane chain, 2.14 nm), was used to estimate the equilibrium constant using eq 1. The estimate of equilibrium log K is ~6, which fits comfortably in the range of solute-sorbent equilibria that are commonly reported for SPE.[50,51]

Elution Solvent Optimization. After developing a DMF-magnetic bead-SPE method, we turned our attention to optimization of elution solvents. Although there are macroscale (robotic) systems that can perform automated elution solvent optimization in SPE,[52−54] we are not aware of any publications describing microfluidic systems with this capacity. DMF seems well suited for this task because of its ability to generate custom solvent mixtures on-the-fly. For example, by dispensing unit droplets of neat water, methanol, and acetonitrile from reservoirs, solvents can be combined and mixed in appropriate proportions on-chip to generate a library of elution solvents with the desired compositions (Figure 3). This library can then be used to determine the optimum elution solvent combination for different analytes.

Two model analytes were used, including sitamaquine as a representative small-molecule drug and angiotensin I as a representative peptide. Although a number of methods have been developed to address the analysis and modeling of mixtures,[55] here we chose to use the chemometric technique known as "design of experiments" (DOE).[56−58] Using a simplex centroid design, seven solvent combinations were chosen and extraction efficiencies evaluated by mass spectrometry (comparing recoveries in each of the seven elution solvent mixtures) for both sitamaquine and angiotensin I. The resulting data was fit with a special cubic function (eq 2) to generate response surface model plots (Figure 4). In the case of sitamaquine, a general trend of increasing extraction efficiency with increasing organic fraction of the elution solvent was observed, with neat methanol yielding a greater efficiency than neat acetonitrile (Figure 4A). These results are in agreement with the trend predicted for sitamaquine solubilities (methanol > acetonitrile > water) according to the Abraham general solvation model.[35] In the case of angiotensin I, a 1:1 acetonitrile/water mixture yields the greatest extraction efficiency (Figure 4B). This result is consistent with the common practice[59] of using aqueous/acetonitrile mobile phases for reversed phase separations of peptides by HPLC. Although the two model analytes used here (sitamaquine and angiotensin I) are well-characterized, we propose that in the future, DMF may be used to automatically optimize extraction protocols for unknown analytes on-the-fly, reducing time and labor associated with method development.

Using the elution solvents optimized through DOE, the extraction efficiencies for sitamaquine and angiotensin I were

DOI: 10.1021/ac504697r
Anal. Chem. 2015, 87, 3902−3910

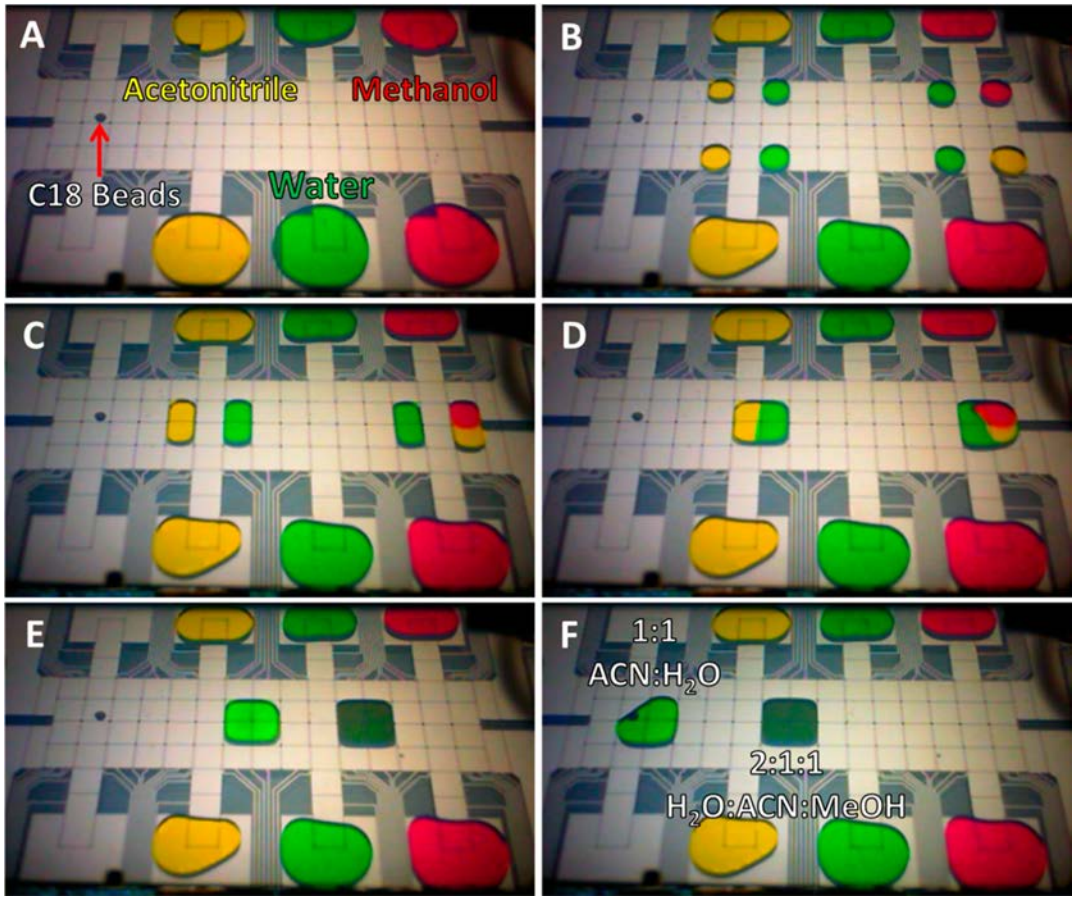

Figure 3. Still frames from a video demonstrating the generation of custom solvent mixtures on DMF. Acetonitrile, methanol, and deionized (DI) water (ACN, MeOH, and H_2O, labeled with yellow, green, and red dyes for visualization) in reservoirs (A) are dispensed in desired proportions (B) and mixed together (C–E) to form elution solvents with desired compositions (in this case, 1:1 ACN:H_2O and 2:1:1 H_2O:ACN:MeOH). Once formed, the droplets can be used to elute analytes from the C18 magnetic beads (F).

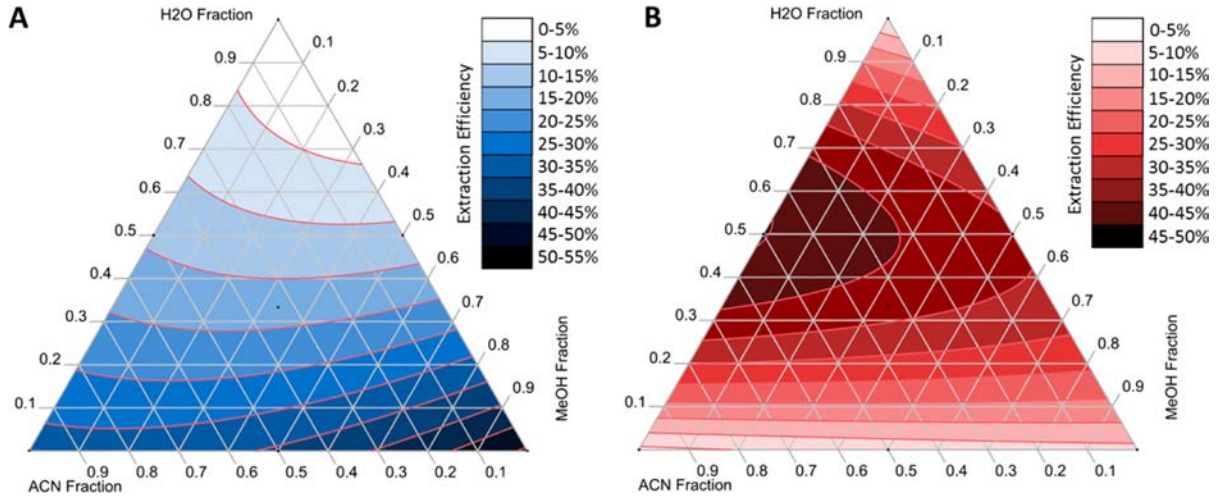

Figure 4. Response surface model plots for extraction efficiency of sitamaquine (1 μg/mL) (A) and angiotensin I (50 μg/mL) (B) in mixtures of DI water (H_2O), acetonitrile (ACN), and methanol (MeOH), where dark color represents increased analyte recovery. Optimal extraction efficiency occurs with 100% methanol for sitamaquine (lower right, A) and 1:1 acetonitrile:water for angiotensin I (left, middle, B). Each plot was generated by measuring the extraction efficiencies (using mass spectrometry) for each of the seven solvent conditions.

compared between C18 magnetic beads on DMF and the popular commercial SPE product, the C18 ZipTip (EMD Millipore, Billerica, Massachusetts). For both analytes, extraction efficiencies were similar (Figure 5). We speculate that optimization of other parameters (e.g., loading and elution time and volume) may improve the total extraction efficiency in future experiments. Regardless, the data in Figure 5 establish the performance of the new DMF method as being comparable to that of an established microscale SPE technique, and is thus promising for future work in this area.

DOI: 10.1021/ac504697r
Anal. Chem. 2015, 87, 3902–3910

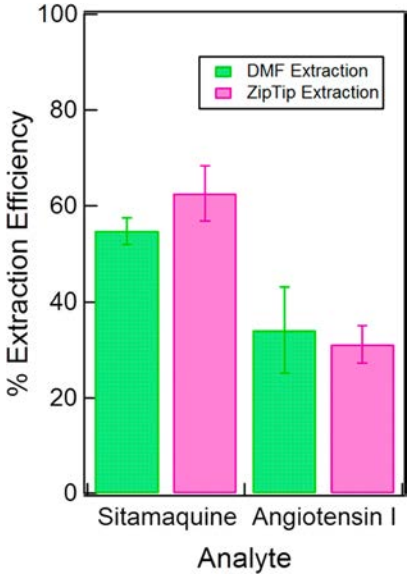

Figure 5. Solid phase extraction efficiencies measured for sitamaquine (1 μg/mL) and angiotensin I (50 μg/mL) using C18 magnetic beads on DMF (green) compared to identical extractions performed using C18 ZipTips (pink). The performance of the extractions is comparable for both analytes. Error bars represent ±1 SD, n = 3.

Sample Fractionation. Fractionation is an important separation technique when multiple analytes of interest are present in a mixture. By selectively desorbing each analyte from the stationary phase, analytes can be collected in separate fractions for individual analysis. In the case of a mixture of sitamaquine and angiotensin I, the DOE results described above suggested that the two model analytes (sitamaquine and angiotensin I) might be selectively eluted under different solvent conditions. As per Figure 4, neat methanol, the optimal elution solvent for sitamaquine, only elutes ~5−10% of angiotensin I. Similarly, 1:1 acetonitrile/water, the optimal elution solvent for angiotensin I, only elutes ~10−15% of sitamaquine. Thus, we hypothesized that two successive elutions, first neat methanol, followed by 1:1 acetonitrile/water, might be used to elute a fraction enriched in sitamaquine followed by a fraction enriched in angiotensin I. As shown in Figure 6, fractionation was largely successful with little (<10%) coelution.

Dried Blood Spot Extraction and Cleanup. As a proof of principle for working with real-world samples, we chose to evaluate the compatibility of the new magnetic bead C18 cleanup method with dried blood spot (DBS) samples. DBS samples are popular because of the capacity to combine detailed analysis with small sample-size requirements.[60] Digital microfluidics has proven to be useful for handling and analyzing DBS samples;[61] however, some pharmaceutical analytes have proven difficult to quantify at low concentrations[36] (likely caused by matrix effects). Here, DBS samples formed from blood spiked with sitamaquine were inserted onto DMF devices where they were extracted and then cleaned-up using the new magnetic bead SPE technique prior to analysis by MS/MS (Figure 7). As

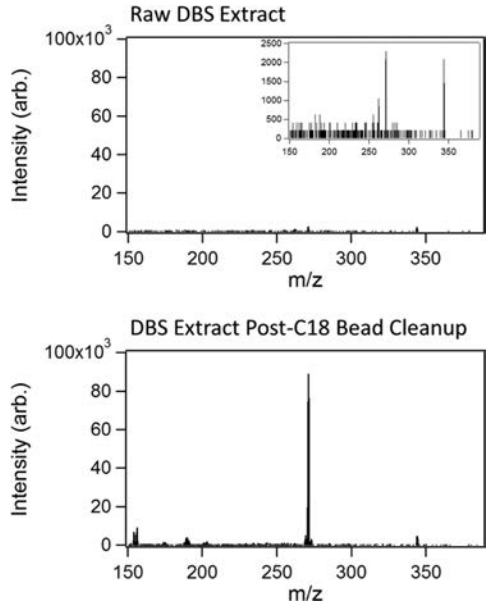

Figure 7. Analysis of sitamaquine from dried blood spots, extracted on-chip. The secondary ion mass spectrum of the raw DBS extract (top) shows little signal for sitamaquine (271 m/z, inset is y-axis-zoomed). After on-chip C18 bead cleanup, the sitamaquine signal is prominent (bottom).

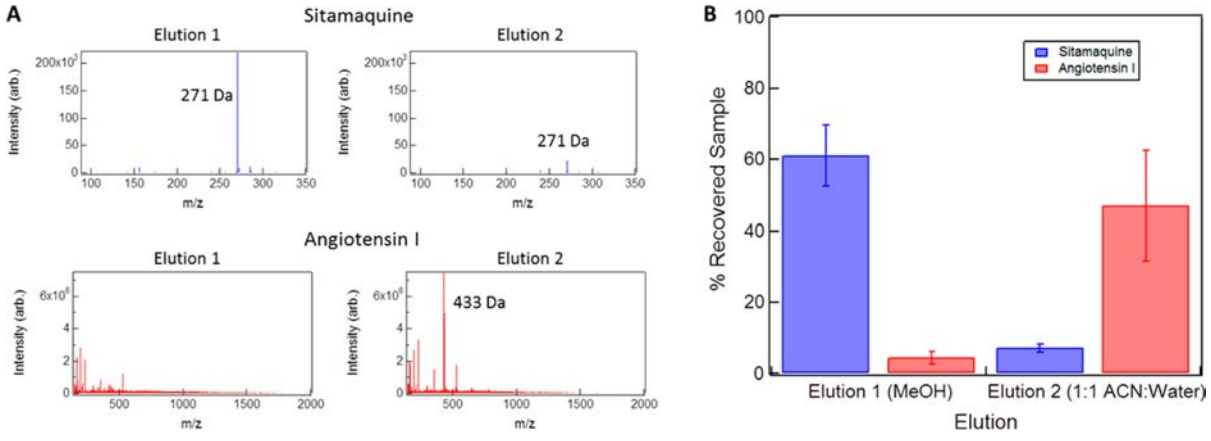

Figure 6. Fractionation of a mixture of sitamaquine (1 μg/mL) (blue) and angiotensin I (50 μg/mL) (red) using DMF-magnetic bead-SPE. Representative mass spectra (A) and % recoveries (B) for elution in methanol (first) and in 1:1: ACN:H_2O (second). Error bars represent ±1 SD, n = 3.

DOI: 10.1021/ac504697r
Anal. Chem. 2015, 87, 3902−3910

shown, samples evaluated postcleanup display a much stronger 344 to 271 m/z transition than "raw" samples that were not cleaned up, likely a function of reduced ionization suppression by matrix components.

We propose that the automated digital microfluidic strategy for fractionation and preconcentration described here represents a useful new option for on-chip sample processing of mixtures. We predict this will be particularly useful for applications such as DBS analysis where samples are limited or precious.[12−14]

CONCLUSION

We have demonstrated a new format for solid phase extraction (SPE) making use of digital microfluidics and functionalized magnetic particles. The new format enables digital microfluidic SPE without compromising the reconfigurability inherent to the technique. Further, the new technique was demonstrated to be compatible with automated solvent optimization and multianalyte fractionation. We propose that this suite of properties will make DMF-magnetic bead-SPE an attractive new tool for a wide range of applications.

AUTHOR INFORMATION

Corresponding Author

*A. R. Wheeler. E-mail: aaron.wheeler@utoronto.ca. Tel: (416) 946 3864. Fax: (416) 946 3865.

Author Contributions

⊥These authors contributed equally to this work.

Notes

The authors declare no competing financial interest.

ACKNOWLEDGMENTS

We thank the Natural Sciences and Engineering Research Council (NSERC), MaRS Innovation, the Ontario Centres of Excellence, AB Sciex, and GlaxoSmithKline for financial support. J.M.M. thanks NSERC and the Ontario Graduate Scholarship (OGS) program for fellowships. A.H.C.N. thanks NSERC for a fellowship. A.R.W. thanks the Canada Research Chair (CRC) Program for a CRC.

REFERENCES

(1) Zwir-Ferenc, A.; Biziuk, M. *Pol. J. Environ. Stud.* **2006**, *15* (5), 677−690.
(2) Veer, V. S.; Pingale, S. G.; Mangaonkar, K. V. *J. Liq. Chromatogr. Relat. Technol.* **2014**, *37* (14), 1953−1967.
(3) Imbert, L.; Dulaurent, S.; Mercerolle, M.; Morichon, J.; Lachatre, G.; Gaulier, J. M. *Forensic Sci. Int.* **2014**, *234*, 132−138.
(4) Wang, R.; Wang, X.; Liang, C.; Ni, C.; Xiong, L.; Rao, Y.; Zhang, Y. *Forensic Sci. Int.* **2013**, *233* (1−3), 304−311.
(5) Raihantaha, M.; Mobasser, S. *Soil Sediment Contam.* **2014**, *23* (7), 703−714.
(6) Ibrahim, W. A. W.; Abd Ali, L. I.; Sulaiman, A.; Sanagi, M. M.; Aboul-Enein, H. Y. *Crit. Rev. Anal. Chem.* **2014**, *44* (3), 233−254.
(7) Bones, J.; Thomas, K. V.; Paull, B. *J. Environ. Monit.* **2007**, *9* (7), 701−707.
(8) Farre, M. L.; Ferrer, I.; Ginebreda, A.; Figueras, M.; Olivella, L.; Tirapu, L.; Vilanova, M.; Barcelo, D. *J. Chromatogr. A* **2001**, *938* (1−2), 187−197.
(9) Anastassiades, M.; Lehotay, S. J.; Stajnbaher, D.; Schenck, F. J. *J. AOAC Int.* **2003**, *86* (2), 412−431.
(10) Paya, P.; Anastassiades, M.; Mack, D.; Sigalova, I.; Tasdelen, B.; Oliva, J.; Barba, A. *Anal. Bioanal. Chem.* **2007**, *389* (6), 1697−1714.
(11) Arora, A.; Simone, G.; Salieb-Beugelaar, G. B.; Kim, J. T.; Manz, A. *Anal. Chem.* **2010**, *82* (12), 4830−4847.
(12) Chueh, B.-h.; Li, C.-W.; Wu, H.; Davison, M.; Wei, H.; Bhaya, D.; Zare, R. N. *Anal. Biochem.* **2011**, *411* (1), 64−70.
(13) Kim, M. S.; Kim, T.; Kong, S.-Y.; Kwon, S.; Bae, C. Y.; Choi, J.; Kim, C. H.; Lee, E. S.; Park, J.-K. *PLoS One* **2010**, *5* (5), Article No. e10441.
(14) Kim, J.; Jensen, E. C.; Stockton, A. M.; Mathies, R. A. *Anal. Chem.* **2013**, *85* (16), 7682−7688.
(15) Kutter, J. P.; Jacobson, S. C.; Ramsey, J. M. *J. Microcolumn Sep.* **2000**, *12* (2), 93−97.
(16) Ekstrom, S.; Wallman, L.; Helldin, G.; Nilsson, J.; Marko-Varga, G.; Laurell, T. *J. Mass Spectrom.* **2007**, *42* (11), 1445−1452.
(17) Li, J. J.; LeRiche, T.; Tremblay, T. L.; Wang, C.; Bonneil, E.; Harrison, D. J.; Thibault, P. *Mol. Cell. Proteomics* **2002**, *1* (2), 157−168.
(18) Oleschuk, R. D.; Shultz-Lockyear, L. L.; Ning, Y. B.; Harrison, D. J. *Anal. Chem.* **2000**, *72* (3), 585−590.
(19) Petersen, N. J.; Jensen, H.; Hansen, S. H.; Foss, S. T.; Snakenborg, D.; Pedersen-Bjergaard, S. *Microfluid. Nanofluid.* **2010**, *9* (4−5), 881−888.
(20) Nge, P. N.; Pagaduan, J. V.; Yu, M.; Woolley, A. T. *J. Chromatogr. A* **2012**, *1261*, 129−135.
(21) Wheeler, A. R. *Science* **2008**, *322* (5901), 539−540.
(22) Lee, J.; Moon, H.; Fowler, J.; Schoellhammer, T.; Kim, C. J. *Sens. Actuators, A* **2002**, *95* (2−3), 259−268.
(23) Ng, A. H. C.; Choi, K.; Luoma, R. P.; Robinson, J. M.; Wheeler, A. R. *Anal. Chem.* **2012**, *84* (20), 8805−8812.
(24) Fiddes, L. K.; Luk, V. N.; Au, S. H.; Ng, A. H. C.; Luk, V.; Kumacheva, E.; Wheeler, A. R. *Biomicrofluidics* **2012**, *6* (1).
(25) Luk, V. N.; Fiddes, L. K.; Luk, V. M.; Kumacheva, E.; Wheeler, A. R. *Proteomics* **2012**, *12* (9), 1310−1318.
(26) Lafrenière, N. M.; Shih, S. C. C.; Abu-Rabie, P.; Jebrail, M. J.; Spooner, N.; Wheeler, A. R. *Bioanalysis* **2014**, *6* (3), 307−318.
(27) Kirby, A. E.; Lafreniere, N. M.; Seale, B.; Hendricks, P. I.; Cooks, R. G.; Wheeler, A. R. *Anal. Chem.* **2014**, *86* (12), 6121−6129.
(28) Shih, S. C. C.; Barbulovic-Nad, I.; Yang, X. N.; Fobel, R.; Wheeler, A. R. *Biosens. Bioelectron.* **2013**, *42*, 314−320.
(29) Eydelnant, I. A.; Li, B. B.; Wheeler, A. R. *Nat. Commun.* **2014**, *5*.
(30) Yang, H.; Mudrik, J. M.; Jebrail, M. J.; Wheeler, A. R. *Anal. Chem.* **2011**, *83* (10), 3824−3830.
(31) Mudrik, J. M.; Dryden, M. D. M.; Lafreniere, N. M.; Wheeler, A. R. *Can. J. Chem.* **2014**, *92* (3), 179−185.
(32) Barbulovic-Nad, I.; Yang, H.; Park, P. S.; Wheeler, A. R. *Lab Chip* **2008**, *8* (4), 519−526.
(33) Choi, K.; Ng, A. H. C.; Fobel, R.; Chang-Yen, D. A.; Yarnell, L. E.; Pearson, E. L.; Oleksak, C. M.; Fischer, A. T.; Luoma, R. P.; Robinson, J. M.; Audet, J.; Wheeler, A. R. *Anal. Chem.* **2013**, *85* (20), 9638−9646.
(34) Abraham Descriptor Prediction from SMILES. http://showme.physics.drexel.edu/onsc/models/AbrahamDescriptorsModel001.php (accessed December 12, 2014).
(35) Abraham, M. H.; Smith, R. E.; Luchtefeld, R.; Boorem, A. J.; Luo, R.; Acree, W. E. *J. Pharm. Sci.* **2010**, *99* (3), 1500−1515.
(36) Shih, S. C. C.; Yang, H.; Jebrail, M. J.; Fobel, R.; McIntosh, N.; Al-Dirbashi, O. Y.; Chakraborty, P.; Wheeler, A. R. *Anal. Chem.* **2012**, *84*, 3731−3738.
(37) Sista, R.; Hua, Z. S.; Thwar, P.; Sudarsan, A.; Srinivasan, V.; Eckhardt, A.; Pollack, M.; Pamula, V. *Lab Chip* **2008**, *8* (12), 2091−2104.
(38) Sista, R. S.; Eckhardt, A. E.; Srinivasan, V.; Pollack, M. G.; Palanki, S.; Pamula, V. K. *Lab Chip* **2008**, *8* (12), 2188−2196.
(39) Vergauwe, N.; Witters, D.; Ceyssens, F.; Vermeir, S.; Verbruggen, B.; Puers, R.; Lammertyn, J. *J. Micromech. Microeng.* **2011**, *21* (5).
(40) Emani, S.; Sista, R.; Loyola, H.; Trenor, C. C., III; Pamula, V. K.; Emani, S. M. *Blood Coagulation Fibrinolysis* **2012**, *23* (8), 760−768.
(41) Tsaloglou, M.-N.; Jacobs, A.; Morgan, H. *Anal. Bioanal. Chem.* **2014**, *406* (24), 5967−5976.
(42) Ng, A. H. C.; Lee, M.; Choi, K.; Fischer, A. T.; Robinson, J. M.; Wheeler, A. R. *Clin. Chem.* **2015**, *61* (2), 420−429.

DOI: 10.1021/ac504697r
Anal. Chem. 2015, 87, 3902−3910

(43) Shah, G. J.; Kim, C. J. *J. Microelectromech. Syst.* **2009**, *18* (2), 363−375.
(44) Kumar, P. T.; Toffalini, F.; Witters, D.; Vermeir, S.; Rolland, F.; Hertog, M. L. A. T. M.; Nicolai, B. M.; Puers, R.; Geeraerd, A.; Lammertyn, J. *Sens. Actuators, B* **2014**, *199*, 479−487.
(45) Mei, N.; Seale, B.; Ng, A. H. C.; Wheeler, A. R.; Oleschuk, R. *Anal. Chem.* **2014**, *86* (16), 8466−8472.
(46) Zimmer, D.; Pickard, V.; Czembor, W.; Muller, C. *J. Chromatogr. A* **1999**, *854* (1−2), 23−35.
(47) Luk, V. N.; Mo, G. C. H.; Wheeler, A. R. *Langmuir* **2008**, *24* (12), 6382−6389.
(48) Au, S. H.; Kumar, P.; Wheeler, A. R. *Langmuir* **2011**, *27* (13), 8586−8594.
(49) Sarvothaman, M. K.; Kim, K. S.; Seale, B.; Brodersen, P. M.; Walker, G. C.; Wheeler, A. R. *Adv. Funct. Mater.* **2015**, *25*, 506−515.
(50) Amin, A. S.; Al-Attas, A. S. *J. Saudi Chem. Soc.* **2012**, *16* (4), 451−459.
(51) Jonker, M. T. O.; Koelmans, A. A. *Environ. Sci. Technol.* **2001**, *35* (18), 3742−3748.
(52) Solid Phase Extraction Solutions. http://www.gilson.com/en/AI/Categories/9/#.VGy2efnF-84 (accessed November 19, 2014).
(53) Fu, S. L.; Lewis, J. *J. Anal. Toxicol.* **2008**, *32* (4), 292−297.
(54) Janiszewski, J. S.; Swyden, M. C.; Fouda, H. G. *J. Chromatogr. Sci.* **2000**, *38* (6), 255−258.
(55) StatSoft, Inc. *Electronic Statistics Textbook*; StatSoft: Tulsa, OK, 2013. http://www.statsoft.com/textbook/ (accessed December 8, 2014).
(56) Synaridou, M.-E. S.; Sakkas, V. A.; Stalikas, C. D.; Albanis, T. A. *J. Chromatogr. A* **2014**, *1348* (0), 71−79.
(57) Sayar, O.; Aboufazeli, F.; Reza Lotfi Zadeh Zhad, H.; Sadeghi, O.; Karimi, M.; Najafi, E. *Curr. Neuropharmacol.* **2014**, *10* (4), 512−521.
(58) Coscolla, C.; Navarro-Olivares, S.; Marti, P.; Yusa, V. *Talanta* **2014**, *119*, 544−552.
(59) Hühmer, A. F. R.; Aced, G. I.; Perkins, M. D.; Gürsoy, R. N.; Jois, D. S. S.; Larive, C.; Siahaan, T. J.; Schöneich, C. *Anal. Chem.* **1997**, *69* (12), 29−58.
(60) Spooner, N.; Lad, R.; Barfield, M. *Anal. Chem.* **2009**, *81* (4), 1557−1563.
(61) Jebrail, M. J.; Yang, H.; Mudrik, J. M.; Lafreniere, N. M.; McRoberts, C.; Al-Dirbashi, O. Y.; Fisher, L.; Chakraborty, P.; Wheeler, A. R. *Lab Chip* **2011**, *11* (19), 3218−3224.

DOI: 10.1021/ac504697r
Anal. Chem. 2015, 87, 3902−3910